Development/Plasticity/Repair

Lynx1 Limits Dendritic Spine Turnover in the Adult Visual Cortex

Mari Sajo,[1,2,3,4,5] **Graham Ellis-Davies,**[2,5] **and Hirofumi Morishita**[1,2,3,4,5]

[1]Department of Psychiatry, [2]Department of Neuroscience, [3]Department of Ophthalmology, [4]Mindich Child Health and Development Institute, and [5]Friedman Brain Institute, Icahn School of Medicine at Mount Sinai, New York, New York 10029

Dendritic spine turnover becomes limited in the adult cerebral cortex. Identification of specific aspects of spine dynamics that can be unmasked in adulthood and its regulatory molecular mechanisms could provide novel therapeutic targets for inducing plasticity at both the functional and structural levels for robust recovery from brain disorders and injuries in adults. Lynx1, an endogenous inhibitor of nicotinic acetylcholine receptors, was previously shown to increase its expression in adulthood and thus to limit functional ocular dominance plasticity in adult primary visual cortex (V1). However, the role of this "brake" on spine dynamics is not known. We examined the contribution of Lynx1 on dendritic spine turnover before and after monocular deprivation (MD) in adult V1 with chronic *in vivo* imaging using two-photon microscopy and determined the spine turnover rate of apical dendrites of layer 5 (L5) and L2/3 pyramidal neurons in adult V1 of Lynx1 knock-out (KO) mice. We found that the deletion of Lynx1 doubled the baseline spine turnover rate, suggesting that the spine dynamics in the adult cortex is actively limited by the presence of Lynx1. After MD, adult Lynx1-KO mice selectively exhibit higher rate of spine loss with no difference in gain rate in L5 neurons compared with control wild-type counterparts, revealing a key signature of spine dynamics associated with robust functional plasticity in adult V1. Overall, Lynx1 could be a promising therapeutic target to induce not only functional, but also structural plasticity at the level of spine dynamics in the adult brain.

Key words: dendritic spine; Lynx1; plasticity; visual cortex

Significance Statement

Dendritic spine turnover becomes limited in the adult cortex. In mouse visual cortex, a premier model of experience-dependent plasticity, we found that the deletion of Lynx1, a nicotinic "brake" for functional plasticity, doubled the baseline spine turnover in adulthood, suggesting that the spine dynamics in the adult cortex is actively limited by Lynx1. After visual deprivation, spine loss, but not gain rate, remains higher in adult Lynx1 knock-out mice than in control wild-type mice, revealing a key signature of spine dynamics associated with robust functional plasticity. Lynx1 would be a promising target to induce not only functional, but also structural plasticity at the level of spine dynamics in adulthood.

Introduction

Brain plasticity becomes limited as a function of age (Hensch, 2004; Wandell and Smirnakis, 2009), which restricts recovery from brain disorders and injuries in adults. Identification of the mechanisms that regulate brain plasticity in adulthood could provide therapeutic targets for robust recovery of brain disorders (Mitchell and Sengpiel, 2009; Bavelier et al., 2010).

Neuronal plasticity can be observed, not only at the functional level, but also at the structural level, such as changes in the size of synaptic complexes and spine turnover (gain and loss). Spine turnover has, in particular, key implications of physical rearrangement of circuit connectivity in affecting behaviors (Caroni et al., 2012). Importantly, spine turnover is also known to decline into adulthood (Grutzendler et al., 2002; Holtmaat et al., 2005). However, even in the adult brain, whereas overall turnover is limited, some aspects of spine turnover remain partially plastic. For example, in the mouse primary visual cortex (V1), monocu-

Received Feb. 17, 2016; revised June 29, 2016; accepted July 4, 2016.

Author contributions: M.S., G.E.-D., and H.M. designed research; M.S., G.E.-D., and H.M. performed research; M.S., G.E.-D., and H.M. analyzed data; M.S., G.E.-D., and H.M. wrote the paper.

This work was supported by the National Institutes of Health (Grants EY024918, EY026053, and MH106919 to H.M. and Grants GM053395 and NS067920 to G.E.-D.), the Knights Templar Eye Foundation (H.M. and M.S), the March of Dimes (H.M.), the Whitehall Foundation (H.M.), the Brain and the Behavior Research Foundation (H.M.), and the Uehara Memorial Foundation (M.S.). We thank Jonathan Wachtel, Dr. Kentaro Tao (RIKEN Brain Institute) for providing technical expertise on spine imaging and analysis, Dr. Ataru Igarashi (University of Tokyo) for statistical analysis, Poromendro Burman for animal care, Masato Sadahiro for helpful insights, Dr. Nathaniel Heintz (Rockefeller University) for providing Lynx1 knock-out mice, and all members of the H.M and G.E-D laboratories for discussion.

The authors declare no competing financial interests.

Correspondence should be addressed to either Graham Ellis-Davies, PhD, or Hirofumi Morishita, MD, PhD, Icahn School of Medicine at Mount Sinai. One Gustave L. Levy Place, Box 1230, New York, NY 10029. E-mail: hirofumi.morishita@mssm.edu or graham.davies@mssm.edu.

DOI:10.1523/JNEUROSCI.0580-16.2016

 0270-6474/16/369472-07$15.00/0

lar deprivation (MD), a model of experience-dependent cortical plasticity (Fagiolini et al., 1994; Gordon and Stryker, 1996; Morishita and Hensch, 2008; Espinosa and Stryker, 2012; Levelt and Hübener, 2012; Hübener and Bonhoeffer, 2014), does not affect spine loss rate, but can induce increase in spine gain rate of apical dendrites of layer 5 (L5) pyramidal neurons, even in adult brain (Hofer et al., 2009). However, the full extent of spine turnover dynamics that can potentially be unmasked in the adult brain is not known. Identification of specific aspects of spine dynamics that can be unmasked in the adult brain and their regulatory molecular mechanisms could provide novel therapeutic targets for inducing robust plasticity at both the functional and structural levels.

Recent studies showed that functional plasticity can be unmasked in the adult brain by the removal of molecular "brakes" such as chondroitin sulfate proteoglycan (CSPG), Nogo Receptor R1 (NogoR1), PirB, and Lynx1 using the V1 as a model (Pizzorusso et al., 2002; McGee et al., 2005; Syken et al., 2006; Morishita et al., 2010). One intriguing possibility is that these brakes also limit spine turnover; however, to what extent they affect spine turnover is unclear. Previous studies with NogoR1 knock-out (KO) mice reported mixed results. One study reported that NogoR1 limits baseline spine turnover in adult cortex (Akbik et al., 2013), but another showed that NogoR1 does not affect spine turnover (Park et al., 2014; Stephany et al., 2015). Most importantly, no previous study has examined the role of molecular brakes during visual deprivation when functional plasticity is expressed. It is essential to understand the nature of spine plasticity that can be unmasked by the removal of these brakes to understand the hidden potential of the adult brain to induce spine dynamics for robust recovery in brain disorders.

Here, we examined the contribution of Lynx1 as a representative of molecular brakes for functional plasticity on dendritic spine turnover in adult V1 before and after MD. Lynx1 is an endogenous inhibitor of nicotinic acetylcholine receptors, similar to α-bungarotoxin in snake venom (Miwa et al., 1999), which increases in adulthood to limit functional plasticity actively in mouse V1 (Morishita et al., 2010). Using longitudinal two-photon fluorescence imaging, we found that the removal of Lynx1 increases the baseline spine turnover of apical dendrites of L5 and L2/3 pyramidal neurons in adult V1. In addition, during MD, adult Lynx1-KO mice showed selectively higher loss rate with no difference in gain rate in L5 neurons compared with wild-type (WT), revealing a key signature of spine dynamics associated with robust functional plasticity in adult V1. To our knowledge, our study represents the first investigation of spine dynamics, not only at the baseline level, but also during MD, in mice lacking molecular brakes, providing a novel mechanism constraining spine turnover in the adult brain.

Materials and Methods

Animals. All animal procedures were conducted under protocols reviewed and approved by the Institutional Animal Care and Use Committee guidelines of the Icahn School of Medicine at Mount Sinai. Thy1-EGFP (M-line; Feng et al., 2000) mice, which express EGFP in L2/3 and L5 pyramidal neurons, were purchased from the Jackson Laboratory [B6.Cg-Tg (Thy1-EGFP) Mrs./J] and used as control WT mice. Lynx1-KO mice (Miwa et al., 2006) were gifted from Dr. Nathaniel Heintz at Rochefeller University and bred with M-line mice. All mice were extensively backcrossed to C57BL/6. Male mice were used at 3–7 months old. Before surgery, mice were housed in groups and, after surgery, each mouse was housed separately in standard and uniform cage sizes (199 mm × 391 mm × 160 mm: width × depth × height; GM500, Tecniplast) and maintained on a 12 h light/dark cycle with *ad libitum* access to food and water.

MD. Mice were anesthetized with isoflurane. Eyelid margins were trimmed with iris scissors and then sutured shut. After performing MD, mice were returned to their home cages and their suture conditions were checked daily until the imaging session.

Surgery. Mice were deeply anesthetized with isoflurane. Mice were then head-fixed on a stereotaxic frame (Narishige). After shaving the hair, a midline incision of the scalp was made by scissors. The periosteum tissue was removed and the metal frame was implanted with dental cement. The next day, mice were deeply anesthetized with an intraperitoneal injection of ketamine (0.10 mg g^{-1} body weight)/xylazine (0.01 mg g^{-1} body weight) mixture and head-fixed with metal frame (CF-10; Narishige). Once anesthetized, mice were subcutaneously injected with dexamethasone (2 mg g^{-1} body weight). Then, areas were marked in the designated stereotactic coordinates for the binocular zone of V1 (3.0 mm lateral and 0.5 mm anterior from lambda). Craniotomy was performed using a micro drill. The skull was removed gently and intact dura was covered with a drop of HEPES ACSF. A sterile 5 mm glass coverslip was placed over the exposed area and sealed with Krazy Glue and dental cement. Imaging began after a 2- to 3-week recovery period as described previously (Crowe and Ellis-Davies, 2014).

Two-photon in vivo *imaging.* For imaging sessions, animals were anesthetized with isoflurane. Two-photon imaging was performed with a Prairie Technologies Ultima microscope and PrarieView software. All images were taken with 20× water-immersion objective (Zeiss W Plan-APOCHROMAT, 1.0 numerical aperture). A mode-locked Ti:sapphire laser (Chameleon Ultra II; Coherent) was used to generate two-photon excitation, with power at the back aperture in the range of 10–50 mW depending on depth. A pixel dwell time of 4 μs with a frame size of 512 × 512 pixels was used. Dendritic spine images were acquired up to a depth of 100 μm at a magnification of 6× zoom and taken in 0.5 μm *z*-steps. Surface vasculature was used for imaging same region. To confirm the location of the binocular zone, flavoprotein autofluorescent imaging was performed in some experiments (Tohmi et al., 2006; Husson et al., 2007). Endogenous green fluorescent images (128 × 128 pixels) were recorded 3.0 mm lateral and 0.5 mm anterior from lambda as a binocular zone and 2.5 mm lateral and 1.0 mm anterior from lambda as a monocular zone of V1 through a cranial window by two-photon microscopy. Images were taken while mice were given visual stimulation to the ipsilateral eye repeatedly over 20 s. As a control, the ipsilateral eye was covered during visual stimulation.

Image analysis. ImageJ was used to analyze all images. *Z*-stacks for branching point analysis were constructed using the ZStackProject function in ImageJ. Only well isolated neurons were analyzed for branching-point analysis. For dendritic spine analysis, the TurboReg plug-in in ImageJ was used for motion correction. Then, the Kalman stack filter plug-in was used to smooth the images. Vaa3D was used to analyze in three dimensions. Dendritic spines were classified as a protrusion from the dendritic shaft at least 0.4 μm (Holtmaat et al., 2009). In L5, a total of 22 dendrites of 11 cells from 5 WT mice and 28 dendrites of 13 cells from eight Lynx1-KO mice were chronically imaged. In L2/3, total of 21 dendrites of 10 cells from five WT mice, 15 dendrites of 10 cells from seven Lynx1-KO mice were chronically imaged. Per mouse, one to three cells were imaged. The spine turnover rate of each cell was calculated after counting the number of gained spines, lost spines, and total spines between each imaging session from one to three dendrites per cell. Gain rate was calculated by dividing the number of gain spines by the number of total spines. Loss rate was calculated by dividing the number of lost spines by the number of total spines. Baseline gain and loss rate per cell were calculated by averaging the rates of days 0–4 and days 4–8 sessions. Spine density was measured by determining the number of spines present per unit length of apical dendrite. Relative density was calculated by dividing spine density by original density at day 0. For flavoprotein imaging analysis, all images during recording period were stacked and the average intensity of imaging fields was calculated. The response to visual stimulation of the ipsilateral eye was normalized by average intensity of controls. This relative response was compared between the binocular zone and the monocular zone.

Statistics. Data were analyzed by two-tailed Student's *t* tests unless otherwise noted. For both gain and loss of WT and Lynx1-KO mice groups, comparisons were made by Multivariate ANOVA (MANOVA) using JMP software and IBM SPSS software.

Results

Normal dendritic complexity and spine density of V1 neurons in adult Lynx1-KO mice

To investigate whether Lynx1 regulates general dendritic complexity and dendritic spine density in adult V1 *in vivo*, Lynx1-KO mice were crossed with the Thy1 GFP M line WT mice in which a small number of L5 and L2/3 pyramidal neurons express GFP (Feng et al., 2000). After craniotomy, animals were implanted with a glass window centered over the binocular zone of V1 for chronic imaging (Holtmaat et al., 2009). Two-photon laser scanning microscopy was used to image structures of L5 and L2/3 neurons to compare the dendritic complexity and spine density in adult WT and Lynx1-KO mice. The imaging area was confirmed to be the binocular zone by detecting a significant increase in flavoprotein autofluorescent intensity through a cranial window upon visual stimulation from the ipsilateral eye ($\Delta F/F$: 1.20 ± 0.15% in binocular zone vs 0.17 ± 0.13% in monocular zone, $p < 0.01$, Student's *t* test, $n = 3$ mice).

The number of dendritic branches were counted after neurons were reconstructed in three dimensions (Fig. 1*A*,*D*). The number of branching points was not significantly different between Lynx1-KO and WT mice in L5 neurons (13.11 ± 1.19 in Lynx1-KO: $n = 9$ cells from 6 mice vs 13.00 ± 0.87 in WT: $n = 7$ cells from 5 mice, $p = 0.94$, Student's *t* test; Fig. 1*B*) and in L2/3 neurons (9.50 ± 1.89 in Lynx1-KO: $n = 4$ cells from 3 mice vs 10.50 ± 1.60 in WT: $n = 6$ cells from 4 mice, $p = 0.70$, Student's *t* test; Fig. 1*E*). The spine density of apical dendrites was also comparable between adult Lynx1-KO and WT mice in L5 neurons (spine counts/μm: 0.31 ± 0.016 in Lynx1-KO: $n = 13$ cells from 8 mice vs 0.29 ± 0.012 in WT: $n = 11$ cells from 5 mice, $p = 0.55$, Student's *t* test; Fig. 1*C*) and L2/3 neurons (0.35 ± 0.031 in Lynx1-KO: $n = 10$ cells from 7 mice vs 0.34 ± 0.026 in WT: $n = 10$ cells from 5 mice, $p = 0.85$, Student's *t* test; Fig. 1*F*). These observations suggest that Lynx1 deletion does not alter the gross morphology of L5 and L2/3 pyramidal neurons.

Increased baseline dendritic spine turnover of V1 neurons in adult Lynx1-KO mice

Once we were sure that Lynx1 did not alter basic neuronal structures, we repeatedly imaged the same dendritic regions every 4 d in the superficial 100 μm of binocular V1 in adult Lynx1-KO and WT mice to determine how Lynx1 regulates spine turnover in adult V1. We analyzed the number of spines gained and lost between two imaging sessions. Baseline rates per cell were calculated by averaging the rates of the days 0–4 and the days 4–8 sessions. In L5 neurons, the spine turnover rate was higher in Lynx1-KO mice for both spine gain rate (15.05 ± 0.61% in Lynx1-KO mice: $n = 13$ cells from 8 mice vs 7.97 ± 0.29% in WT mice: $n = 11$ cells from 5 mice: $p < 0.01$ by, Student's *t* test) and spine loss rate (14.42 ± 0.58% in Lynx1-KO mice vs 7.79 ± 0.50% in WT mice: $p < 0.01$ by, Student's *t* test) (Fig. 2*A*,*B*). In L2/3 neurons, the spine turnover rate was also higher in Lynx1-KO mice for both gain rate (11.37 ± 0.29% in Lynx1-KO mice: $n = 10$ cells from 7 mice vs 5.97 ± 0.26% in WT mice, $n = 10$ cells from 5 mice: $p < 0.01$, Student's *t* test) and loss rate (11.90 ± 0.41% in Lynx1-KO mice vs 6.73 ± 0.26% in WT mice, $p < 0.01$, Student's *t* test) (Fig. 2*C*,*D*). Importantly, whereas both spine gain and loss rates were almost doubled in adult Lynx1-KO mice compared with WT mice in L5 and L2/3 neurons, the elevated rates were comparable between spine gain rate and loss rate in Lynx1-KO mice (L5 $p = 0.462$, L2/3 $p = 0.298$, Student's *t* test) without affecting the spine density in Lynx1-KO mice (Fig. 1*C*,*F*). These results suggest that Lynx1 limits the global dendritic spine turnover in adult V1.

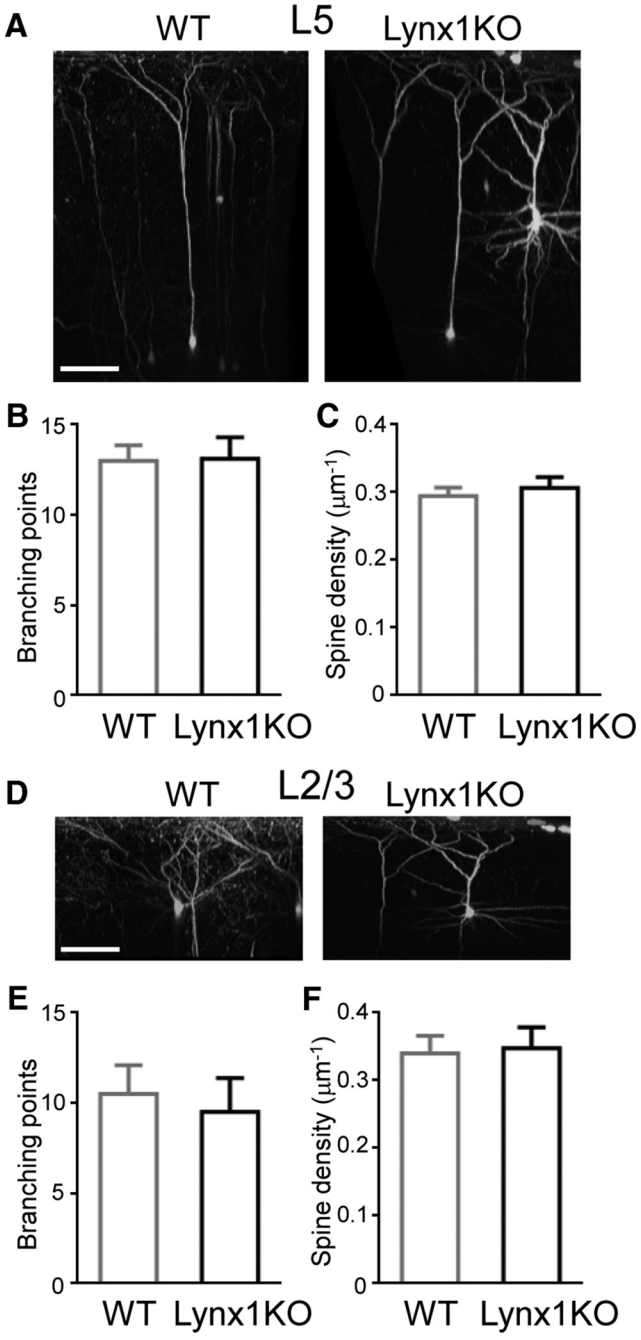

Figure 1. Normal dendritic complexity and spine density of L5 and L2/3 V1 neurons in adult Lynx1-KO mice. ***A***, 3D reconstruction of *in vivo* two-photon images of L5 pyramidal neuron in binocular zone of V1 of adult WT and Lynx1-KO mouse. Scale bar, 100 μm. ***B***, Number of branching points of apical dendrite of L5 neurons (WT: $n = 7$ cells from 5 mice, KO: $n = 9$ cells from 6 mice). ***C***, Spine density (number of spines per micrometer) of L5 neurons (WT: $n = 11$ cells from 5 mice, KO: $n = 13$ cells from 8 mice). ***D***, 3D reconstruction of two-photon images of L2/3 pyramidal neurons. ***E***, Number of branching points of apical dendrite of L2/3 neurons (WT: $n = 6$ cells from 4 mice, KO: $n = 4$ cells from 3 mice). ***F***, Spine density (number of spines per micrometer) of L2/3 neurons (WT: $n = 10$ cells from 5 mice, KO: $n = 10$ cells from 7 mice). One to three dendrites were imaged from each cell to count the total spines in each cell. Data are presented as mean ± SEM.

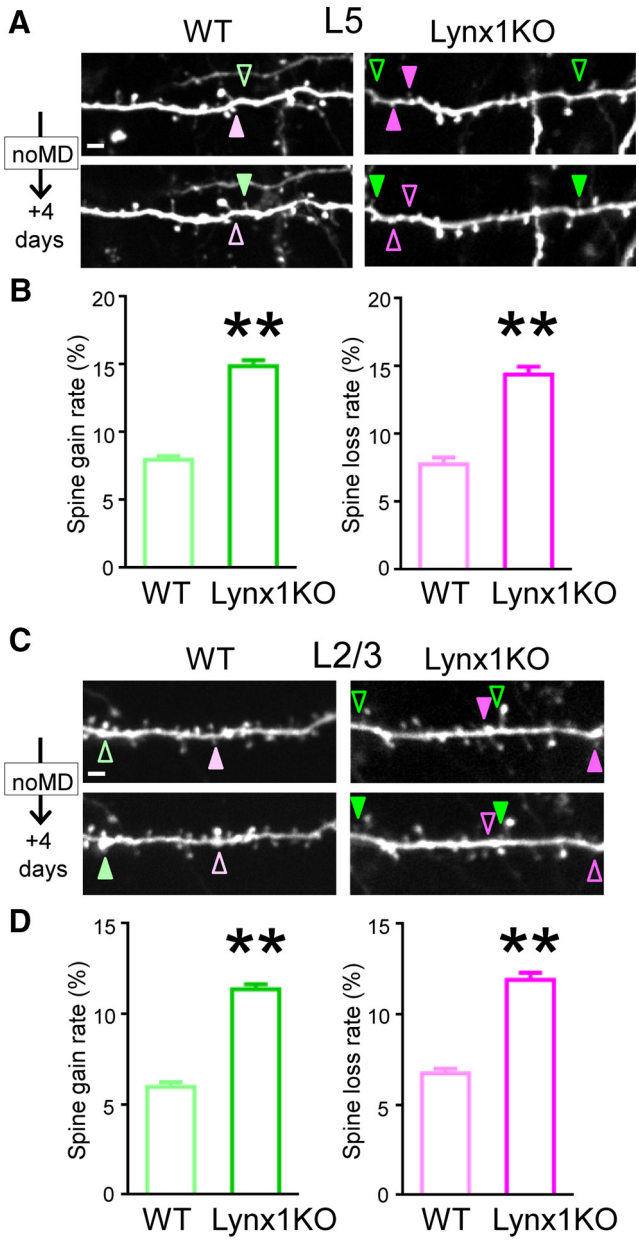

Figure 2. Spine turnover of adult L5 and L2/3 V1 neurons is higher in Lynx1-KO mice than in WT mice. ***A***, Repeated imaging of dendritic segments of adult L5 V1 pyramidal neurons over 4 d in adult WT mice and Lynx1-KO mice. Light green (WT) and green (KO) arrowheads indicate gained spine. Light magenta (WT) and magenta (KO) arrowheads indicate lost spine. Scale bar, 5 μm. One to three dendrites were imaged from each cell to count total, gained, and lost spines in each cell. ***B***, Spine gain and loss rate of adult L5 V1 pyramidal neurons over 4 d are significantly higher in adult Lynx1-KO mice than in WT mice (WT: $n = 11$ cells from 5 mice, KO: $n = 13$ cells from 8 mice). ***C***, Repeated imaging of dendritic segment of adult L2/3 V1 pyramidal neuron. ***D***, Spine gain and loss rate of adult L2/3 V1 pyramidal neurons over 4 d were significantly higher in adult Lynx1-KO mice than in WT mice (WT: $n = 10$ cells from 5 mice, KO: $n = 10$ cells from 7 mice). Data are presented as mean ± SEM. $^{**}p < 0.01$.

Most newly formed spines are typically known to become lost quickly and therefore are called "transient" spines, whereas the rest of spines become "persistent" spines (Holtmaat et al., 2005). In our experiments, spines were classified as transient if they disappeared within 8 d and as persistent if they were observed over 8 d. In adult Lynx1-KO mice, transient spines were increased (L5: 6.59 ± 0.68% in Lynx1-KO vs 2.31 ± 0.44% in WT, $n =$ 11–12 cells each from 5–7 mice each, $p < 0.01$, Student's t test, L2/3: 4.73 ± 0.47% in Lynx1-KO vs 2.12 ± 0.44% in WT, $n =$ 9–10 cells from 5–6 mice each, $p < 0.01$, Student's t test) and persistent spines were decreased (L5: 77.37 ± 1.66% in Lynx1-KO vs 85.99 ± 0.89% in WT, $n = 12$ cells each from 5–7 mice each, $p < 0.01$, Student's t test, L2/3: 80.78 ± 0.94% in Lynx1-KO vs 89.55 ± 0.66% in WT, 9–10 cells from 5–6 mice, $p < 0.01$, Student's t test). These results suggest that elevated spine turnover in Lynx1-KO mice can be explained by a relative increase of the transient spine pool.

Spine loss, but not gain rate, of L5 neurons is higher in adult Lynx1-KO mice than in WT mice during MD

We next examined the role of Lynx1 on spine dynamics when experience is altered by MD. A previous study in adult WT mice reported that the spine gain rate was higher than the spine loss rate after 4 d of MD in L5 pyramidal neurons due to an increase in spine gain from the baseline level (Hofer et al., 2009). To test to what extent this pattern of spine dynamics during MD is different between Lynx1-KO mice and WT mice, we imaged dendritic spines after 4 d of MD (Fig. 3*A*). Only those dendritic images that were clearly imaged during whole imaging sessions were included in analysis and quantification. In L5 neurons, the loss rate remained higher in Lynx1-KO mice compared with WT mice during and even after 4 d MD (13.27 ± 0.77% in Lynx1-KO: $n = 12$ cells from 7 mice vs 8.74 ± 0.56% in WT: $n = 11$ cells from 5 mice, $p < 0.01$, Student's t test; Fig. 3*B*). In contrast, the gain rate was comparable between the two genotypes (16.68 ± 0.67% in Lynx1-KO: $n = 12$ cells from 7 mice vs 15.68 ± 0.66% in WT: $n =$ 11 cells from 5 mice, $p = 0.30$, Student's t test; Fig. 3*B*).

Next, to examine the impact of MD on spine turnover rates, we compared spine turnover rates before and after MD within each genotypic group (Fig. 3*C*). The spine gain rate of WT mice was significantly increased after MD [day 12 vs day 8: $p < 0.001$. 95% confidence interval (95%CI): −9.754 to −5.463, *post hoc* pairwise comparisons using Bonferroni modification], which is consistent with a previous study (Hofer et al., 2009), whereas no change was detected in Lynx1-KO mice. In contrast, spine loss rate of Lynx1-KO mice was significantly decreased after MD (day 12 vs day 8: $p =$ 0.047. 95%CI: 0.019–4.262, *post hoc* pairwise comparisons using Bonferroni modification; Fig. 3*C*), whereas no change was observed in WT mice (see the detailed statistical analysis in the legend to Fig. 3). To determine whether the MD-induced change in spine dynamics affects the spine number, we analyzed relative spine density. Spine density was normalized to that of day 0 of imaging. WT mice showed the expected increase in relative density after MD (1.08 ± 0.011 in day 12 vs 1.01 ± 0.0082 in day 8, $n = 11$ cells from 5 mice, $p < 0.01$, Student's t test). In contrast, Lynx1-KO mice did not show a statistically significant difference in relative density after MD (1.05 ± 0.014 in day 12 vs 1.02 ± 0.015 in day 8, $n = 12$ cells from 8 mice, $p =$ 0.34, Student's t test). We also did not observe differences in relative spine density at day 12 between WT and Lynx1-KO ($p = 0.19$, Student's t test). Collectively, these genotypic differences underscore the significance of the spine loss during MD and its regulation by Lynx1.

Dendritic spine turnover of L2/3 neurons is higher in adult Lynx1-KO mice than in WT mice during MD

Finally, we examined the spine turnover of L2/3 neurons after MD in adult Lynx1-KO mice. A previous study in juvenile WT mice reported a decrease in spine density after MD in L2/3 neurons (Mataga et al., 2004), but not in adult WT mice (Hofer et al., 2009). Only those dendritic images that were clearly imaged during whole imaging sessions were included in analysis and quantification. In adult Lynx1-KO mice, both the gain and loss rate remained higher during

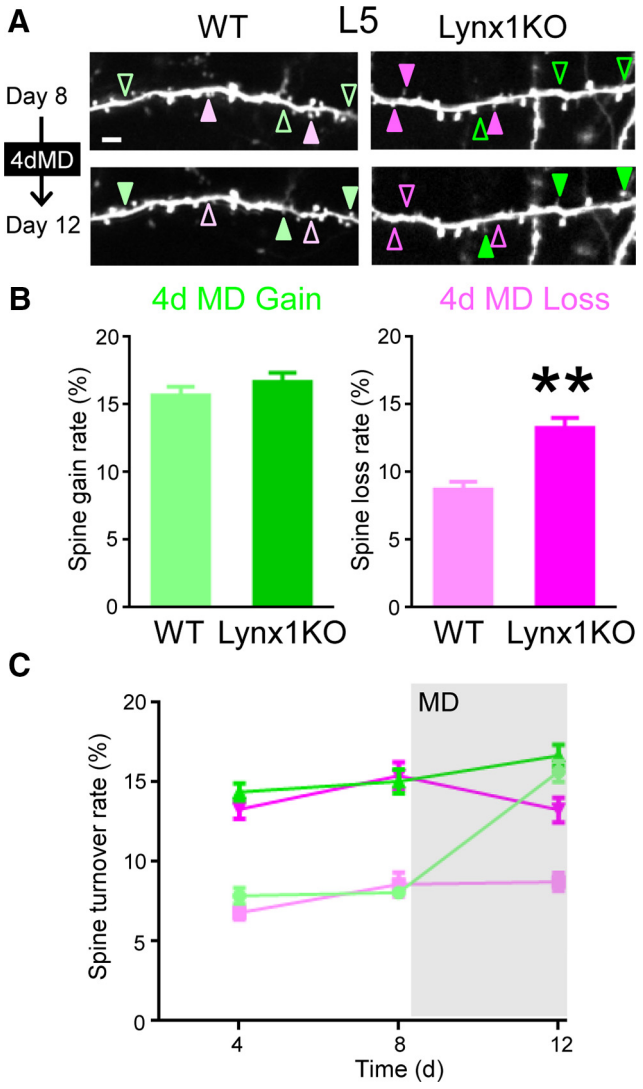

Figure 3. Spine loss rate of adult L5 V1 neurons is higher in Lynx1-KO mice than in WT mice during MD. ***A***, Repeated imaging of dendritic segment of adult L5 neurons before (day 8) and after (day 12) MD (4dMD). Light green (WT) and green (KO) arrowheads indicate spine gain. Light magenta (WT) and magenta (KO) arrowheads indicate spine loss. One to three dendrites were imaged from each cell to count total, gained, and lost spines in each cell. Scale bar, 5 μm. ***B***, Spine gain and loss rate after 4 d of MD. Spine loss rate was significantly higher in adult Lynx1-KO mice than in WT mice (WT: $n = 11$ cells from 5 mice, KO: $n = 12$ cells from 7 mice). $^{**}p < 0.01$, Student's t test. ***C***, Spine turnover rates over 4 d were plotted as a function of time. Light green, light magenta, green, and magenta indicate WT gain, WT loss, Lynx1-KO gain, and Lynx1-KO loss, respectively. MD occurred right after day 8 imaging. Initial statistical analysis was done using MANOVA, in which interactions among three factors: genotype (knock out/wild type), type (gain/loss), and time (day 4/day 8/day 12) were assessed. Turnover rates significantly differed between genotypes (KO vs WT, df = 42, exact F value = 113.18, $p < 0.0001$). Interaction between genotype and type was not statistically significant (df = 42, exact F value = 1.216, $p = 0.277$). Therefore, effects for "loss" or "gain" value were independently assessed with the generalized linear model, in which "genotype" and "time" were adopted as fixed-effects variables and "cell" was adopted as a random-effect variable. For loss rate, both "time" and "genotype" were statistically significant. (df = 52, $F = 4.901$ and $p = 0.011$ for time and $F = 125.843$ and $p < 0.001$ for genotype, respectively). As the result of *post hoc* pairwise comparisons using Bonferroni modification, loss values for KO were significantly different between day 12 and day 8 ($p = 0.047$. 95%CI: 0.019 – 4.262), whereas no other comparisons were statistically significant (KO: days 4 – 8, days 4 –12 and WT: days 4 – 8, days 4 –12, days 8 –12). For gain rate, both "time" and "genotype" were statistically significant (df = 52, $F = 43.439$ and $p < 0.001$ for time and $F = 92.171$ and $p < 0.001$ for genotype, respectively). As the result of *post hoc* pairwise comparisons using Bonferroni modification, gain values for WT significantly differed in between day 8 and day 12 ($p < 0.001$. 95%CI: −9.754 to −5.463), whereas there was no significant difference for KO (days 8 –12). Data are presented as mean ± SEM.

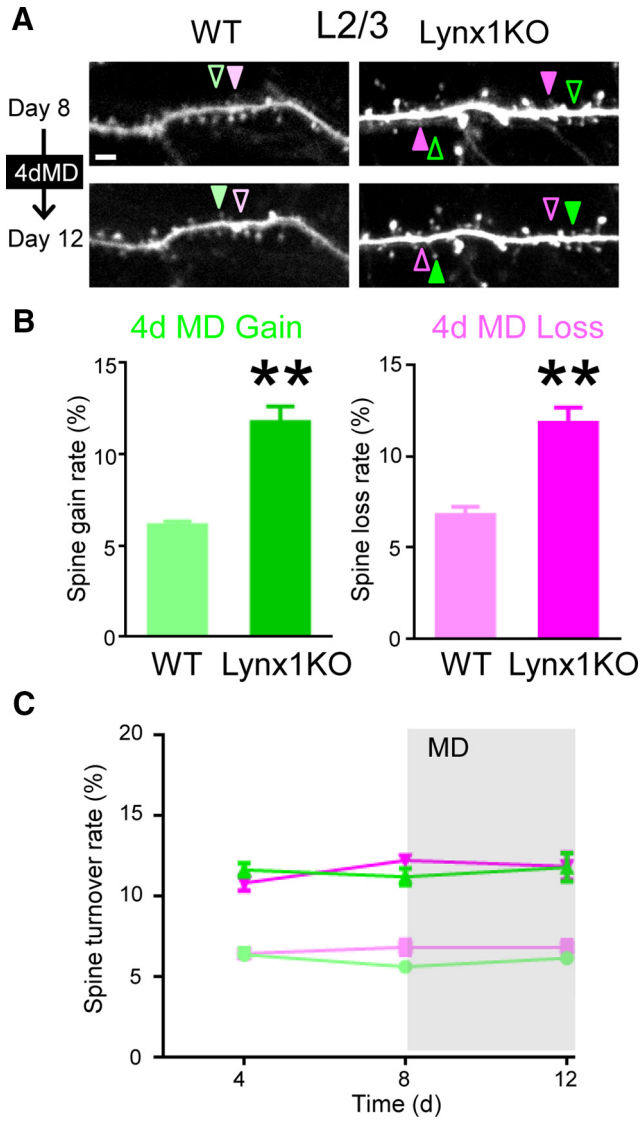

Figure 4. Spine gain and loss rates of adult L2/3 V1 neurons are higher in Lynx1-KO mice than in WT mice during MD. ***A***, Repeated imaging of dendritic segment of adult L2/3 V1 neurons before (day 8) and after (day 12) MD. Light green (WT) and green (KO) arrowheads indicate spine gain. Light magenta (WT) and magenta (KO) arrowheads indicate spine loss. One to three dendrites were imaged from each cell to count total, gained, and lost spines in each cell. Scale bar, 5 μm. ***B***, Spine gain and loss rate after 4 d of MD (4dMD). Spine loss rate was significantly higher in adult Lynx1-KO mice than in WT mice (WT: $n = 10$ cells from 5 mice, KO: 9 cells from 6 mice). $^{**}p < 0.01$, Student's t test. ***C***, Spine turnover rates over 4 d were plotted as a function of time. Light green, light magenta, green, and magenta indicate WT gain, WT loss, Lynx1-KO gain, and Lynx1-KO loss, respectively. MD occurred after day 8 imaging. Initial statistical analysis was done using MANOVA, in which interactions among three factors: genotype (knock out/wild type), type (gain/loss), and time (day 4/day 8/day 12) were assessed. Turnover rates significantly differed between genotype (KO vs WT, df = 35, exact F value = 164.860, $p < 0.0001$). The interaction between genotype and type was not statistically significant (df = 34, exact F value = 0.464, $p = 0.500$). Therefore, effects for the loss or gain value were assessed independently with ageneralized linear model, in which genotype and time were adopted as fixed-effect variables and cell was adopted as a random-effect variable. Genotype was statistically significant. (df = 42, $F = 126.217$ and $p < 0.0001$ for loss, df = 42, $F = 199.452$ and $p < 0.0001$ for gain), but time was not significant (df = 42, $F = 1.708$ and $p = 0.193$ for loss, df = 42, $F = 1.047$ and $p = 0.360$ for gain). *Post hoc* pairwise comparisons using Bonferroni modification did not detect any significant difference in any comparisons for loss or gain values. Data are presented as mean ± SEM.

MD compared with those of adult WT mice during MD (gain: 11.76 ± 0.87%, loss:11.83 ± 0.84% in Lynx1-KO: $n = 9$ cells from 6 mice vs gain: 6.12 ± 0.21%, loss: 6.79 ± 0.16% in WT: $n = 10$ cells from 5 mice, $p < 0.01$, Student's t test; Fig. 4*A*,*B*). There was no

significant difference before and after MD in each group (Fig. 4*C*, MANOVA, see the detailed statistical analysis in Fig. 4 legend). Relative density was also not significant different before and after MD in each group (Lynx1-KO: 1.00 ± 0.009 at day 12 vs 1.00 ± 0.006 at day 8, $p = 0.91$, WT: 0.98 ± 0.011 at day 12 vs 0.99 ± 0.006 at day 8, $p = 0.79$, Student's *t* test). Collectively, our data suggest that Lynx1 limits the global spine turnover in L2/3 V1 neurons in adulthood regardless of the presence of MD.

Discussion

We investigated the role of Lynx1 on spine turnover as a representative of molecular brakes on plasticity both before and after MD in adult V1. We found that the removal of Lynx1 increases the baseline spine turnover, suggesting that spine dynamics in the adult cortex are actively limited by the presence of Lynx1 and that robust spine turnover can be effectively unmasked by the removal of this molecular brake. We also showed that, during MD, adult Lynx1-KO mice exhibit a selectively higher loss rate with no difference in gain rate in L5 neurons compared with adult WT, revealing a key signature of spine dynamics associated with robust functional plasticity in adult V1. Overall, Lynx1 could be a promising target to induce not only functional but also structural plasticity at the level of spine dynamics. Our study provides a key template for future studies to examine the general role of Lynx1 on spine turnover in other brain regions. Genetic deletion of Lynx1 or overexpression of a dominant-negative soluble version of Lynx1 was shown to improve motor performance and learning (Miwa and Walz, 2012). Interestingly, a decrease in spine gain in neurons proximal to amyloid-β plaques was reported recently in one animal model of neurodegenerative disorder (Dorostkar et al., 2015; Herms and Dorostkar, 2016). It could be fruitful in future studies to assess whether a therapeutic Lynx1 polypeptide is useful in treating memory dysfunctions across multiple modalities by rescuing spine turnover deficits.

At the baseline level, we demonstrated that the spine turnover rate is higher in adult Lynx1-KO mice than in adult WT mice. Because Lynx1 expression increases from adolescence to adulthood, when spine turnover decreases in WT mice (Holtmaat et al., 2005; Morishita et al., 2010), removal of Lynx1 may leave the spine dynamics comparable to the juvenile mice level. This suggests the potential for restoring, not only functional, but also structural, plasticity in the adult brain. Similar to the removal of Lynx1, environmental enrichment, which can restore juvenile-like functional plasticity, is also known to elevate the turnover of dendritic spines of L2/3 and L5 pyramidal neurons (Jung and Herms, 2014). It could be important to study the impact of other molecular brakes or behavioral interventions on spine dynamics to conclude whether increased spine turnover is a common feature of restored functional plasticity in adult brain.

We also demonstrated that, after MD, whereas the spine gain rate becomes comparable between adult Lynx1-KO mice and adult WT mice in L5 neurons due to an MD-induced increase in spine gain in WT mice (Hofer et al., 2009), spine loss rate remains significantly higher in Lynx1-KO mice compared with WT matched controls in both L5 and L2/3 neurons. These results suggest greater spine loss as a better correlate of elevated functional plasticity in adult Lynx1-KO mice. Interestingly, in adult Lynx1-KO neurons, MD induced a reduction in spine loss rate, with no change in gain rate, in contrast to adult WT L5 neurons, in which it is known that MD increases the spine gain rate with no change in the loss rate (Hofer et al., 2009). Given that juvenile mouse barrel cortex also similarly exhibits whisker-trimming-induced reduction of spine loss (Zuo et al., 2005), the experience-dependent changes observed in Lynx1-KO mice reflects characteristics of juvenile, but not adult, WT brain. It should be noted that the magnitude of the MD-dependent changes in spine loss rate in Lynx1-KO is a rather moderate one; smaller than the MD-dependent increase in gain rate in WT mice. In fact, the MD-dependent effect was only captured within the 4 d interval imaging sessions between days 8 and 12, but not between longer 8 d interval sessions, between days 4 and 12, when an increase in within-subject variability is expected. Such moderate change may reflect the heterogeneous nature of preexisting spines' response to MD. Future study with more frequent and longer total imaging sessions would allow detailed temporal characterization of preexisting spines to determine whether there is any differential effect of MD across the different types of spines. In contrast to L5 neurons, in L2/3 neurons of adult Lynx1-KO mice, MD did not induce changes in spine turnover nor spine density as in adult WT mice. This pattern is distinct from that of juvenile WT mice, in which a previous study has demonstrated MD-dependent decrease in the spine density of L2/3 pyramidal cells in the visual cortex (Mataga et al., 2004), suggesting that the nature of spine dynamics in adult Lynx1-KO mice does not fully resemble the juvenile state.

How can the altered spine dynamics in Lynx1-KO mice contribute to the elevated functional ocular dominance plasticity in adult Lynx1-KO mice (Morishita et al., 2010)? In adult Lynx1-KO mice, our previous study showed that MD increased the V1 visual response of the open ipsilateral eye and decreased the response of the deprived contralateral eye (Bukhari et al., 2015). Genotypically higher spine loss during MD of L2/3 and L5 neurons in Lynx1-KO mice may contribute to a decrease in deprived contralateral eye response if spines with dominant response to the deprived contralateral eye are eliminated preferentially during MD. Elevated spine formation rate in L2/3 neurons in Lynx1-KO mice may also contribute to functional plasticity (i.e., and increase in open ipsilateral eye response) if spines with dominant response to ipsilateral open eyes are formed preferentially during MD. Recent advancement in functional imaging at a single-spine level will allow future studies to address this question (Chen et al., 2013).

How can Lynx1 deletion lead to a general increase in the spine turnover? Because Lynx1 is an endogenous inhibitor of nicotinic acetylcholine receptors, its removal leads to hypernicotinic signaling, which in turn elevates Ca^{2+}. Ca^{2+} influx through nAChRs can then activate MAPK and CaMKII/IV pathways known to be critical for the formation of stable dendritic filopodial extensions (Wu et al., 2001) in part through CaMK-mediated Rac1 activation to inhibit actin de-polymerization factor cofilin, thereby increasing actin polymerization for spine formation (Lai and Ip, 2013). Ca^{2+} elevations also play an important role in spine shrinkage and loss. An elevated intracellular Ca^{2+} level activates calcineurin, a Ca^{2+}/calmodulin-dependent protein phosphatase necessary for activity-induced spine shrinkage (Pontrello et al., 2012). Consistent with the role of Lynx1 in spine dynamics, Fragile X, an upstream regulator of *Lynx1* translation (Darnell et al., 2011), is known to limit baseline turnover rate similar to Lynx1 (Pan et al., 2010). Tissue plasminogen activator, which is known to be regulated downstream of Lynx1 (Bukhari et al., 2015), can also increase the spine motility in V1 (Oray et al., 2004).

An alternation of the excitatory–inhibitory balance at the network level (Caroni et al., 2012) could also contribute to the observed changes in spine dynamics in Lynx1-KO mice. Lynx1 is expressed in both excitatory and inhibitory neurons and enhancement of inhibition by diazepam treatment abolishes the ocular dominance plasticity in adult Lynx1-KO mice (Morishita et al., 2010). Recent studies suggest that GABAergic signaling is involved in spine plasticity. GABA-Aα1 KO mice showed impaired spine maturation in adulthood (Heinen et al., 2003).

GABAergic inhibition suppresses local dendritic Ca^{2+} transients and promotes activity-dependent loss of spines (Hayama et al., 2013). Cell-type-specific manipulation of Lynx1 expression in combination with *in vivo* imaging of excitatory and inhibitory synapses will allow dissection of the role of Lynx1 at the network level in future studies.

References

Akbik FV, Bhagat SM, Patel PR, Cafferty WB, Strittmatter SM (2013) Anatomical plasticity of adult brain is titrated by Nogo Receptor 1. Neuron 77:859–866. CrossRef Medline

Bavelier D, Levi DM, Li RW, Dan Y, Hensch TK (2010) Removing brakes on adult brain plasticity: from molecular to behavioral interventions. J Neurosci 30:14964–14971. CrossRef Medline

Bukhari N, Burman PN, Hussein A, Demars MP, Sadahiro M, Brady DM, Tsirka SE, Russo SJ, Morishita H (2015) Unmasking Proteolytic Activity for Adult Visual Cortex Plasticity by the Removal of Lynx1. J Neurosci 35:12693–12702. CrossRef Medline

Caroni P, Donato F, Muller D (2012) Structural plasticity upon learning: regulation and functions. Nat Rev Neurosci 13:478–490. CrossRef Medline

Chen TW, Wardill TJ, Sun Y, Pulver SR, Renninger SL, Baohan A, Schreiter ER, Kerr RA, Orger MB, Jayaraman V, Looger LL, Svoboda K, Kim DS (2013) Ultrasensitive fluorescent proteins for imaging neuronal activity. Nature 499:295–300. CrossRef Medline

Crowe SE, Ellis-Davies GC (2014) Longitudinal in vivo two-photon fluorescence imaging. J Comp Neurol 522:1708–1727. CrossRef Medline

Darnell JC, Van Driesche SJ, Zhang C, Hung KY, Mele A, Fraser CE, Stone EF, Chen C, Fak JJ, Chi SW, Licatalosi DD, Richter JD, Darnell RB (2011) FMRP stalls ribosomal translocation on mRNAs linked to synaptic function and autism. Cell 146:247–261. CrossRef Medline

Dorostkar MM, Zou C, Blazquez-Llorca L, Herms J (2015) Analyzing dendritic spine pathology in Alzheimer's disease: problems and opportunities. Acta Neuropathol 130:1–19. CrossRef Medline

Espinosa JS, Stryker MP (2012) Development and plasticity of the primary visual cortex. Neuron 75:230–249. CrossRef Medline

Fagiolini M, Pizzorusso T, Berardi N, Domenici L, Maffei L (1994) Functional postnatal development of the rat primary visual cortex and the role of visual experience: dark rearing and monocular deprivation. Vis Res 34:709–720. CrossRef Medline

Feng G, Mellor RH, Bernstein M, Keller-Peck C, Nguyen QT, Wallace M, Nerbonne JM, Lichtman JW, Sanes JR (2000) Imaging neuronal subsets in transgenic mice expressing multiple spectral variants of GFP. Neuron 28:41–51. CrossRef Medline

Gordon JA, Stryker MP (1996) Experience-dependent plasticity of binocular responses in the primary visual cortex of the mouse. J Neurosci 16:3274–3286. Medline

Grutzendler J, Kasthuri N, Gan WB (2002) Long-term dendritic spine stability in the adult cortex. Nature 420:812–816. CrossRef Medline

Hayama T, Noguchi J, Watanabe S, Takahashi N, Hayashi-Takagi A, Ellis-Davies GC, Matsuzaki M, Kasai H (2013) GABA promotes the competitive selection of dendritic spines by controlling local Ca2+ signaling. Nat Neurosci 16:1409–1416. CrossRef Medline

Heinen K, Baker RE, Spijker S, Rosahl T, van Pelt J, Brussaard AB (2003) Impaired dendritic spine maturation in GABAA receptor alpha1 subunit knock out mice. Neuroscience 122:699–705. CrossRef Medline

Hensch TK (2004) Critical period regulation. Annu Rev Neurosci 27:549–579. CrossRef Medline

Herms J, Dorostkar MM (2016) Dendritic spine pathology in neurodegenerative diseases. Annu Rev Pathol 11:221–250. CrossRef Medline

Hofer SB, Mrsic-Flogel TD, Bonhoeffer T, Hübener M (2009) Experience leaves a lasting structural trace in cortical circuits. Nature 457:313–317. CrossRef Medline

Holtmaat AJ, Trachtenberg JT, Wilbrecht L, Shepherd GM, Zhang X, Knott GW, Svoboda K (2005) Transient and persistent dendritic spines in the neocortex in vivo. Neuron 45:279–291. CrossRef Medline

Holtmaat A, Bonhoeffer T, Chow DK, Chuckowree J, De Paola V, Hofer SB, Hübener M, Keck T, Knott G, Lee WC, Mostany R, Mrsic-Flogel TD, Nedivi E, Portera-Cailliau C, Svoboda K, Trachtenberg JT, Wilbrecht L (2009) Long-term, high-resolution imaging in the mouse neocortex through a chronic cranial window. Nat Protoc 4:1128–1144. CrossRef Medline

Hübener M, Bonhoeffer T (2014) Neuronal plasticity: beyond the critical period. Cell 159:727–737. CrossRef Medline

Husson TR, Mallik AK, Zhang JX, Issa NP (2007) Functional imaging of primary visual cortex using flavoprotein autofluorescence. J Neurosci 27:8665–8675. CrossRef Medline

Jung CK, Herms J (2014) Structural dynamics of dendritic spines are influenced by an environmental enrichment: an in vivo imaging study. Cereb Cortex 24:377–384. CrossRef Medline

Lai KO, Ip NY (2013) Structural plasticity of dendritic spines: the underlying mechanisms and its dysregulation in brain disorders. Biochim Biophys Acta 1832:2257–2263. CrossRef Medline

Levelt CN, Hübener M (2012) Critical-period plasticity in the visual cortex. Annu Rev Neurosci 35:309–330. CrossRef Medline

Mataga N, Mizuguchi Y, Hensch TK (2004) Experience-dependent pruning of dendritic spines in visual cortex by tissue plasminogen activator. Neuron 44:1031–1041. CrossRef Medline

McGee AW, Yang Y, Fischer QS, Daw NW, Strittmatter SM (2005) Experience-driven plasticity of visual cortex limited by myelin and Nogo receptor. Science 309:2222–2226. CrossRef Medline

Mitchell DE, Sengpiel F (2009) Neural mechanisms of recovery following early visual deprivation. Philos Trans R Soc Lond B Biol Sci 364:383–398. CrossRef Medline

Miwa JM, Walz A (2012) Enhancement in motor learning through genetic manipulation of the Lynx1 gene. PLoS One 7:e43302. CrossRef Medline

Miwa JM, Ibanez-Tallon I, Crabtree GW, Sánchez R, Sali A, Role LW, Heintz N (1999) lynx1, an endogenous toxin-like modulator of nicotinic acetylcholine receptors in the mammalian CNS. Neuron 23:105–114. CrossRef Medline

Miwa JM, Stevens TR, King SL, Caldarone BJ, Ibanez-Tallon I, Xiao C, Fitzsimonds RM, Pavlides C, Lester HA, Picciotto MR, Heintz N (2006) The prototoxin lynx1 acts on nicotinic acetylcholine receptors to balance neuronal activity and survival in vivo. Neuron 51:587–600. CrossRef Medline

Morishita H, Hensch TK (2008) Critical period revisited: impact on vision. Curr Opin Neurobiol 18:101–107. CrossRef Medline

Morishita H, Miwa JM, Heintz N, Hensch TK (2010) Lynx1, a cholinergic brake, limits plasticity in adult visual cortex. Science 330:1238–1240. CrossRef Medline

Oray S, Majewska A, Sur M (2004) Dendritic spine dynamics are regulated by monocular deprivation and extracellular matrix degradation. Neuron 44:1021–1030. CrossRef Medline

Pan F, Aldridge GM, Greenough WT, Gan WB (2010) Dendritic spine instability and insensitivity to modulation by sensory experience in a mouse model of fragile X syndrome. Proc Natl Acad Sci U S A 107:17768–17773. CrossRef Medline

Park JI, Frantz MG, Kast RJ, Chapman KS, Dorton HM, Stephany CÉ, Arnett MT, Herman DH, McGee AW (2014) Nogo receptor 1 limits tactile task performance independent of basal anatomical plasticity. PLoS One 9:e112678. CrossRef Medline

Pizzorusso T, Medini P, Berardi N, Chierzi S, Fawcett JW, Maffei L (2002) Reactivation of ocular dominance plasticity in the adult visual cortex. Science 298:1248–1251. CrossRef Medline

Pontrello CG, Sun MY, Lin A, Fiacco TA, DeFea KA, Ethell IM (2012) Cofilin under control of beta-arrestin-2 in NMDA-dependent dendritic spine plasticity, long-term depression (LTD), and learning. Proc Natl Acad Sci U S A 109:E442–451. CrossRef Medline

Stephany CE, Frantz MG, McGee AW (2015) Multiple roles for Nogo Receptor 1 in visual system plasticity. Neuroscientist. In press.

Syken J, Grandpre T, Kanold PO, Shatz CJ (2006) PirB restricts ocular-dominance plasticity in visual cortex. Science 313:1795–1800. CrossRef Medline

Tohmi M, Kitaura H, Komagata S, Kudoh M, Shibuki K (2006) Enduring critical period plasticity visualized by transcranial flavoprotein imaging in mouse primary visual cortex. J Neurosci 26:11775–11785. CrossRef Medline

Wandell BA, Smirnakis SM (2009) Plasticity and stability of visual field maps in adult primary visual cortex. Nat Rev Neurosci 10:873–884. CrossRef Medline

Wu GY, Deisseroth K, Tsien RW (2001) Spaced stimuli stabilize MAPK pathway activation and its effects on dendritic morphology. Nat Neurosci 4:151–158. CrossRef Medline

Zuo Y, Yang G, Kwon E, Gan WB (2005) Long-term sensory deprivation prevents dendritic spine loss in primary somatosensory cortex. Nature 436:261–265. CrossRef Medline